Inorg. Chem. **2005**, *44*, 5706–5712

New Phosphorescent Polynuclear Cu(I) Compounds Based on Linear and Star-Shaped 2-(2′-Pyridyl)benzimidazolyl Derivatives: Syntheses, Structures, Luminescence, and Electroluminescence

Wen Li Jia,[†] Theresa McCormick,[†] Ye Tao,[‡] Jian-Ping Lu,[‡] and Suning Wang*,[†]

Department of Chemistry, Queen's University, Kingston, Ontario K7L 3N6, Canada, and Institute for Microstructural Science, National Research Council of Canada, Ottawa K1A 0R6, Canada

Received April 3, 2005

Four dinuclear and trinuclear Cu(I) complexes that contain 2-(2′-pyridyl)benzimidazolyl derivative ligands including 1,4-bis[2-(2′-pyridyl)benzimidazolyl]benzene (1,4-bmb), 1,3-bis[2-(2′-pyridyl)benzimidazolyl]benzene (1,3-bmb), 1,3,5-tris[2-(2′-pyridyl)benzimidazolyl]benzene (tmb), and 4,4′-bis[2-(2′-pyridyl)benzimidazolyl]biphenyl (bmbp) have been synthesized. The formulas of these complexes are $[Cu_2(1,4\text{-bmb})(PPh_3)_4][BF_4]_2$ (**1**), $[Cu_2(1,3\text{-bmb})(PPh_3)_4][BF_4]_2$ (**2**), $[Cu_3(tmb)(PPh_3)_6][BF_4]_3$ (**3**), and $[Cu_2(bmbp)(PPh_3)_4][BF_4]_2$ (**4**), respectively. The crystal structures of **2**–**4** have been determined by single-crystal X-ray diffraction analyses. The Cu(I) ions in the complexes have a distorted tetrahedral geometry. For **3**, two structural isomers (syn and anti) resulted from two different orientations of the three 2-(2′-pyridyl)benzimidazolyl chelating units were observed in the crystal lattice. Variable-temperature ^{1}H NMR experiments established the presence of syn and anti isomers for **1**–**3** in solution which interconvert at ambient temperature. Complexes **1**–**4** have a weak MLCT absorption band in the 350–450 nm region and display a yellow-orange emission when irradiated by UV light. One unexpected finding is that the yellow-orange emission of complexes **1**–**4** has a very long decay lifetime (∼200 μs) at 77 K. An electroluminescent (EL) device using **4** as the emitter and PVK as the host was fabricated. However, the long decay lifetime of the copper complexes may limit their applications as phosphorescent emitters in EL devices.

Introduction

Phosphorescent transition metal complexes have a wide range of potential applications such as photochemical catalysts,[1] chemical sensors/probes,[2] sensitizers in photovoltaic devices,[3] and emitters in organic light emitting diodes (OLEDs).[4,5] Earlier investigations on phosphorescent compounds as emitters for OLEDs focus mostly on Ir(III), Pt(II), and Ru(II) complexes. Highly efficient electroluminescent devices using Pt(II) or Ir(III) complexes as phosphorescent dopants have been illustrated by a number of research groups.

* To whom correspondence should be addressed. E-mail: wangs@chem.queensu.ca.

[†] Queen's University.

[‡] National Research Council of Canada.

(1) (a) Houlding, V. H.; Miskowski, V. M. *Coord. Chem. Rev.* **1991**, *111*, 145. (b) Pettijohn, C, N.; Jochnowitz, E. B.; Chuong, B.; Nagle, J. K.; Vogler, A. *Coord. Chem. Rev.* **1998**, *171*, 85. (c) Yersin, H.; Humbs, W.; Strasser, J. *Coord. Chem. Rev.* **1997**, *159*, 325. (d) Paw, W.; Cummings, S. D.; Mansour, M. A.; Connick, W. B.; Gieger, D. K.: Eisenberg, R. *Coord. Chem. Rev.* **1998**, *171*, 125. (e) McGarrah, J. E.; Kim, Y. J.; Hissler, M.; Eisenberg, R. *Inorg. Chem.* **2001**, *40*, 4510. (f) Vlèek, A., Jr. *Coor. Chem. Rev.* **2000**, *200*−*202*, 933.

(2) (a) Chassot, L.; Müller, E.; von Zelewsky, A. *Inorg. Chem.* **1984**, *23*, 4249. (b) Sandrini, D.; Maestri, M.; Balzani, V.; Chassot, L.; von Zelewsky, A. *J. Am. Chem. Soc.* **1987**, *109*, 3107. (c) Vogler, A.; Kunkely, H. *Coord. Chem. Rev.* **1998**, *177*, 81. (d) Wan, K. T.; Che, C. M.; Cho, K. C. *J. Chem. Soc., Dalton Trans.* **1991**, 1077. (e) Che, C. M.; Wan, K. T.; He, L. T.; Poon, C. K.; Yam, V. W. W. *J. Chem. Soc., Dalton Trans.* **1989**, 2011. (f) Wan, K. T.; Che, C. M. *J. Chem. Soc., Chem. Commun.* **1990**, 140.

(3) (a) O'Regan, B.; Grätzel, M. *Nature* **1991**, *353*, 737. (b) Grätzel, M., *J. Photochem. Photobiol. A*: *Chem.* **2004**, *164*, 3.

(4) (a) Shen, Z.; Burrows, P. E.; Bulovic, V.; Borrest, S. R.; Thompson, M. E. *Science* **1997**, *276*, 2009. (b) Baldo, M. A.; Lamansky, S.; Burrows, P.; Thompson, M. E.; Forrest, S. R. *Appl. Phys. Lett.* **1999**, *75*, 5. (c) Kwong, R. C.; Sibley, S.; Dubovoy, T.; Baldo, M.; Forrest, S. R.; Thompson, M. E. *Chem. Mater*. **1999**, *11*, 3709 (d) Adachi, C.; Baldo, M. A.; Forrest, S. R.; Thompson, M. E. *Appl. Phys. Lett*. **2000**, *77*, 904. (e) Lamansky, S.; Djurovich, P.; Murphy, D.; Abdel-Razzaq, F.; Lee, H. E.; Adachi, C.; Burrows, P. E.; Forrest, S. R.; Thompson, M. E. *J. Am. Chem. Soc*. **2001**, *123*, 4304. (f) Liu, Q. D.; Thorne, L.; Kozin, I.; Song, D.; Seward, C.; D'Iorio, M.; Tao, Y.; Wang, S. *J. Chem. Soc., Dalton Trans.* **2002**, 3234. (g) Lu, W.; Mi, B. X., Chan, M. C. W.; Hui, Z.; Zhu, N.; Lee, S. T.; Che, C. M. *Chem. Commun.* **2002**, 206.

(5) (a) Rudmann, H.; Shimada, S.; Rubner, M. F. *J. Am. Chem. Soc.* **2002**, *124*, 4918. (b) Bernhard, S.; Barron, J. A.; Houston, P. L.; Abruña, H. D.; Ruglovksy, J. L.; Gao, X.; Malliaras, G. G. *J. Am. Chem. Soc.* **2002**, *124*, 13624. (c) Buda, M.; Kalyzuzhny, G.; Bard, A. *J. Am. Chem. Soc.* **2002**, *124*, 6090.

10.1021/ic0504893 CCC: $30.25
Published on Web 07/14/2005

Phosphorescent Cu(I) complexes have been demonstrated recently by Wang and co-workers to be promising phosphorescent emitters in OLEDs,[6] which prompted our interest in the development of new phosphorescent Cu(I) compounds. The previously reported phosphorescent Cu(I) complexes are mononuclear green emitters that contain a phenanthroline *N*,*N*-chelate (or its derivative) and two phosphine donors, which have been shown by McMillin and co-workers to play a key role in stabilizing the Cu(I) center.[7] Except for the phenanthroline-based Cu(I) complexes, phosphorescent Cu(I) compounds that are useful in electroluminescent (EL) devices remain scarce. Our investigation focuses on new dinuclear and trinuclear Cu(I) complexes based on 2-(2′-pyridyl)benzimidazolyl aryl derivative ligands. We have shown recently that the 2-(2′-pyridyl)benzimidazolyl derivative ligands are blue emitters and are effective chelating ligands for metal ions such as Pt(II).[8] Stable red phosphorescent polynuclear Pt(II) complexes based on this class of ligands have been reported recently by us. The red emission from the Pt(II) complexes was attributed to MLCT transitions. The goal of our investigation is to determine if the 2-(2′-pyridyl)benzimidazolyl ligands are capable of producing MLCT phosphorescent emission once they are bound to the Cu(I) center, how efficient is the emission, what is the emission color, and finally what are their uses in OLEDs. The results of our investigation including syntheses, structural characterization, luminescent, and electroluminescent properties of four new polynuclear Cu(I) complexes are presented herein.

Experimental Section

All starting materials were purchased from Aldrich Chemical Co. and used without further purification. Solvents were freshly distilled over appropriate drying reagents. All experiments were carried out under a dry nitrogen atmosphere using standard Schlenk techniques unless otherwise stated. Flash chromatography was carried out on silica (silica gel 60, 70−230 mesh). $^{13}P\{^1H\}$ NMR spectra were recorded on a Bruker Avance 400 or 500 MHz spectrometers. Variable-temperature ^1H NMR spectra for **1**−**3** were recorded on a 500 MHz spectrometer. Excitation and emission spectra were recorded on a Photon Technologies International QuantaMaster Model C-60 spectrometer. Emission lifetime was measured on a Photon Technologies International Phosphorescent spectrometer, Time-master C-631F equipped with a Xenon flash lamp and digital emission photon multiplier tube using band pathway of 5 nm for excitation and 2 nm for emission. Elemental analyses were performed by Canadian Microanalytical Service Ltd., Delta, British Columbia, Canada. Cyclic voltammetry was performed using a BAS CV-50W analyzer with a scan rate of 500 mV s^{-1}. The electrolytic cell used was a conventional three-compartment cell, in which a Pt working electrode, a Pt auxiliary electrode, and a Ag/AgCl reference electrode were employed. The CV measurements were performed at room temperature using 0.10 M tetrabutylammonium hexafluorophosphate (TBAP) as the supporting electrolyte and CH_3CN as the solvent. The ferrocenium/ferrocene couple was used as the internal standard ($E_o = 0.53$ V). Copper(I) complexes, $[Cu(CH_3CN)_4][BF_4]$ and $[Cu(CH_3CN)_2(PPh_3)_2][BF_4]$ were synthesized on the basis of literature procedures.[9] The ligands, 1,4-Bis[2-(2′-pyridyl)benzimidazolyl]benzene (1,4-bmb), 4,4′-bis[2-(2′-pyridyl)benzimidazolyl]biphenyl (bmbp), 1,3,5-tris[2-(2′-pyridyl)benzimidazolyl]benzene (tmb), and 1,3-bis-[2-(2′-pyridyl)benzimidazolyl]benzene (1,3-bmb) were synthesized using the methods reported recently by our group.[8]

Synthesis of $[Cu_2(1,4\text{-bmb})(PPh_3)_4][BF_4]_2$ (1). A CH_2Cl_2 (8 mL) solution of $[Cu(CH_3CN)_2(PPh_3)_2]BF_4$ (0.222 g, 0.294 mmol) was mixed with a CH_2Cl_2 (5 mL) solution of 1,4-bmb (0.068 g, 0.147 mmol), and the mixture was stirred for 2 h at room temperature. Then, 2 mL of toluene was successfully layered upon the solution. Slow evaporation of the solvents and diffusion of toluene into the CH_2Cl_2 layer afforded complex **1** as a yellow solid after 2 days (0.201 g, 74% yield). $^{31}P\{^1H\}$ NMR in CD_2Cl_2 (δ, ppm, 298 K): 3.14. ^1H NMR in CD_2Cl_2 (δ, ppm, 298 K): 8.42 (d, $J = 5.0$, 2H), 8.05 (br s, 2H), 7.77 (br s, 4H), 7.55 (br s, 4H), 7.48−7.39 (m, 20 H), 7.28−7.21 (m, 48H). Anal. Calcd. for $C_{102}H_{80}Cu_2B_2F_8N_6P_4 \cdot 0.5CH_2Cl_2$: C, 66.29; H, 4.37; N, 4.53. Found: C, 66.56; H, 4.42; N, 4.80.

Synthesis of $[Cu_2(1,3\text{-bmb})(PPh_3)_4][BF_4]_2$ (2). A solution of 1,3-bmb (0.026 g, 0.055 mmol) in CH_2Cl_2 (5 mL) was mixed with a solution of $[Cu(CH_3CN)_2(PPh_3)_2]BF_4$ (0.082 g, 0.110 mol) in CH_2Cl_2 (5 mL) to produce a yellow solution that was layered with toluene and hexanes. Yellow crystals were obtained after 3 days (0.077 g, 76%). $^{31}P\{^1H\}$ NMR (CD_2Cl_2, δ, ppm, 298 K): 3.36. ^1H NMR in CD_2Cl_2 (δ, ppm, 298 K): 8.40 (br s, 2H), 8.26 (t, $J =$ 8.0, 2H), 8.06 (br s, 2H), 7.83 (d, 8.0, 2H), 7.53−7.17 (m, 72H). Anal. Calcd for $C_{102}H_{80}B_2Cu_2F_8N_6P_4$: C, 67.52; H, 4.44; N, 4.63. Found: C, 67.84; H, 4.38; N, 4.84.

Synthesis of $[Cu_3(tmb)(PPh_3)_6][BF_4]_3$ (3). A solution of tmb (0.025 g, 0.038 mmol) in CH_2Cl_2 (5 mL) was mixed with $[Cu(CH_3CN)_2(PPh_3)_2]BF_4$ (0.086 g, 0.114 mmol) dissolved in CH_2Cl_2 (5 mL) to produce a yellow solution. The solution was layered with toluene and hexanes. Yellow and orange crystals were obtained after 4 days (0.065 g, 62%). $^{31}P\{^1H\}$ NMR (CD_2Cl_2, δ, ppm, 298 K): 3.33. ^1H NMR in CD_2Cl_2 (δ, ppm, 298 K): 8.40 (br s, 3H), 7.92−7.7.76 (m, 3H), 7.73−7.58 (m, 6H), 7.53−7.39 (m, 6H), 7.30−7.10 (m, 99H). Anal. Calcd for $C_{150}H_{117}B_3Cu_3F_{12}N_9P_6 \cdot CH_2Cl_2$: 65.54; H 4.30; N, 4.56. Found: C 65.15; H 4.57; N 4.82.

Synthesis of $[Cu_2(bmbp)(PPh_3)_4][BF_4]_2$ (4). A CH_2Cl_2 (8 mL) solution of $[Cu(CH_3CN)_2(PPh_3)_2]BF_4$ (0.300 g, 0.40 mmol) was mixed with a $CHCl_3$ (10 mL) solution of bmbp (0.108 g, 0.20 mmol). Toluene was added. Slow evaporation of the solvents afforded complex **4** as yellow crystals after 3 days (0.103 g, 89% yield). $^{31}P\{^1H\}$ NMR (CD_2Cl_2, δ, ppm, 298 K): 3.18. ^1H NMR in CD_2Cl_2 (δ, ppm, 298 K): 8.38 (d, $J = 4.8$, 2H), 8.18 (d, $J = 8.4$, 4H), 7.83 (td, $J = 8.0$, 1.6, 2H), 7.56 (d, $J = 8.4$, 4H), 7.47−7.20 (m, 72H). Anal. Calcd for $C_{108}H_{84}B_2Cu_2F_8N_6P_4$: C, 68.61; H, 4.45; N, 4.45. Found: C, 68.35; H, 4.44; N, 4.48.

X-Ray Crystallographic Analysis. Single crystals of compounds **2**−**4** were obtained from the mixed solvent solution of either toluene/CH_2Cl_2 or toluene/CH_2Cl_2/$CHCl_3$. Attempts to grow single crystals of compound **1** were unsuccessful. Crystals were mounted on glass fibers for data collection. Data were collected on a Siemens P4 single-crystal X-ray diffractometer with a Smart CCD-1000 detector and graphite-monochromated Mo Kα radiation, operating

(6) Zhang, Q.; Zhou, Q.; Cheng, Y.; Wang, L.; Ma, D.; Jing, X.; Wang, F. *Adv. Mater.* **2004**, *16*, 432.
(7) (a) Cuttell, D. G.; Kuang, S. M.; Fanwick, P. E.; McMillin, D. R.; Walton, R. A. *J. Am. Chem. Soc.* **2002**, *124*, 6. (b) Kuang, S. M. Cuttell, D. G.; McMillin, D. R.; Fanwick, P. E.; Walton, R. A. *Inorg. Chem.* **2002**, *41*, 3313.
(8) Liu, Q. D.; Jia, W. L.; Wang, S. *Inorg. Chem.* **2005**, *44*, 1332.
(9) (a) Kubas, G. J. *Inorg. Synth.* **1979**, *19*, 90. (b) Diez, J.; Falagan, S.; Gamasa, P.; Gimeno, J. *Polyhedron* **1988**, *7*, 37.

Table 1. Crystallographic Data for Compounds **2**−**4**

	2	**3**	**4**
formula	$C_{116}H_{96}N_6P_4F_8B_2Cu_2$	$C_{156}H_{126}N_9F_{12}P_6B_3Cl_5Cu_3$	$C_{117}H_{100}N_6F_8B_2Cl_{16}P_4Cu_2$
fw	1998.57	2940.77	2629.77
space group	$P2/c$	$P\bar{1}$	$P\bar{1}$
a, Å	15.941(7)	13.444(4)	10.753(4)
b, Å	10.920(5)	17.235(6)	12.997(5)
c, Å	29.012(13)	30.922(10)	21.737(9)
α, deg	90.00	92.044	96.050(7)
β, deg	98.577(8)	101.857(6)	92.137(8)
γ, deg	90.00	96.359	100.115(7)
V, Å^3	4994(4)	6972(4)	2969(2)
Z	2	2	1
D_{calc}, g cm^{-3}	1.329	1.401	1.471
μ, cm^{-1}	5.58	6.91	8.37
$2\theta_{max}$, deg	56.86	56.72	56.68
no. of reflns measd	34315	42390	17180
no. of reflns used	11660	28402	11686
(R_{int})	(0.1080)	(0.0606)	(0.0335)
no. of params	604	1705	699
final R [$I > 2\sigma(I)$]			
R1[a]	0.0721	0.0991	0.0684
wR2[b]	0.1660	0.2168	0.1659
R (all data)			
R1[a]	0.2471	0.2400	0.1367
wR2[b]	0.2124	0.2692	0.1894
GOF on F^2	0.769	1.014	0.756

[a] $R1 = \sum[|F_o| - |F_c|]/\sum|F_o|$. [b] $wR2 = \{\sum[w(F_o^2 - F_c^2)]/\sum(wF_o^2)\}^{1/2}$. $\omega = 1/[\sigma^2(F_o^2) + (0.075P)^2]$, where $P = [\max(F_o^2,0) + 2F_c^2]/3$.

at 50 kV and 30 mA at 23 °C for **2** and at −93 °C for **3** and **4**. No significant decay was observed for all samples. Data were processed on a PC using the Bruker SHELXTL software package[10] (version 5.10) and were corrected for Lorentz and polarization effects. Compound **2** belongs to the monoclinic space group $P2/c$, while compounds **3** and **4** belong to the triclinic space group $P\bar{1}$. Solvent molecules were located in the crystal lattice for all three compounds. For **2**, each molecule cocrystallizes with two toluene solvent molecules. For **3**, 2.5 CH_2Cl_2 and 0.5 toluene solvent molecules per molecule of **3** were located. For **4**, one toluene, four $CHCl_3$, and two CH_2Cl_2 solvent molecules cocrystallized with each molecule. All toluene solvent molecules in **2**−**4** are disordered and could not be fully modeled. The BF_4 anions in all compounds were also found to display disordering and were refined successfully. One of the phenyl groups of the PPh_3 ligands in **2** and **3** displays rotational disordering. One of the 2-(2′-pyridyl)benzimidazolyl units in **3** (the one that is bound to the Cu(3) atom) is disordered over two sites with 50% occupancy for each site. The disordering of this unit was modeled successfully. However, due to the disordering, the Cu(3)−N bond lengths are not accurate. The biphenyl unit in **4** also displays disordering over two sites with 50% occupancy factor for each site. Most nonhydrogen atoms except the disordered ones in **2**−**4** were refined anisotropically. All hydrogen atoms except those on disordered carbon atoms were calculated, and their contributions in structural factor calculations were included. The crystallographic data are given in Table 1. Selected bond lengths and angles for complexes **2**−**4** are listed in Table 2.

Quantum Yield Measurements. The absolute photoluminescent quantum yields of all Cu(I) complexes doped in PMMA films (20% complex:80% PMMA by weight) were measured at ambient temperature using a commercial fluorimeter in combination with an integration sphere according to the literature procedure.[11]

Table 2. Selected Bond Lengths (Å) and Angles (deg)

		Compound **2**	
Cu(1)−N(2)	2.063(5)	N(2)−Cu(1)−N(1)	78.3(2)
Cu(1)−N(1)	2.176(5)	N(2)−Cu(1)−P(1)	106.70(14)
Cu(1)−P(1)	2.2505(18)	N(1)−Cu(1)−P(1)	116.36(14)
Cu(1)−P(2)	2.2564(19)	N(2)−Cu(1)−P(2)	115.86(13)
		N(1)−Cu(1)−P(2)	105.85(14)
		P(1)−Cu(1)−P(2)	124.66(7)
		Compound **3**	
Cu(1)−N(1)	2.063(6)	N(1)−Cu(1)−N(2)	79.4(2)
Cu(1)−N(2)	2.155(6)	N(1)−Cu(1)−P(3)	112.46(17)
Cu(1)−P(3)	2.234(2)	N(2)−Cu(1)−P(3)	114.34(16)
Cu(1)−P(5)	2.256(2)	N(1)−Cu(1)−P(5)	105.14(17)
Cu(2)−N(4)	2.073(6)	N(2)−Cu(1)−P(5)	105.69(17)
Cu(2)−N(5)	2.124(6)	P(3)−Cu(1)−P(5)	128.68(8)
Cu(2)−P(6)	2.237(3)	N(4)−Cu(2)−N(5)	80.2(2)
Cu(2)−P(4)	2.252(2)	N(4)−Cu(2)−P(6)	116.85(19)
Cu(3)−N(7)	1.951(12)	N(5)−Cu(2)−P(6)	110.94(18)
Cu(3)−P(1)	2.238(3)	N(4)−Cu(2)−P(4)	102.99(18)
Cu(3)−P(2)	2.246(3)	N(5)−Cu(2)−P(4)	108.55(18)
Cu(3)−N(9A)	2.293(13)	P(6)−Cu(2)−P(4)	127.28(9)
		N(7A)−Cu(3)−P(1)	119.1(4)
P(1)−Cu(3)−P(2)	132.93(10)	N(7)−Cu(3)−P(1)	110.0(4)
N(7)−Cu(3)−N(9A)	76.7(5)	N(7A)−Cu(3)−P(2)	103.5(4)
P(1)−Cu(3)−N(9A)	104.5(3)	N(7)−Cu(3)−P(2)	113.7(4)
P(2)−Cu(3)−N(9A)	101.7(3)		
		Compound **4**	
Cu(1)−N(1)	2.062(4)	N(1)−Cu(1)−P(1)	110.56(12)
Cu(1)−N(2)	2.104(5)	N(2)−Cu(1)−P(1)	110.75(12)
Cu(1)−P(1)	2.2466(15)	N(1)−Cu(1)−P(2)	112.86(12)
Cu(1)−P(2)	2.2530(17)	N(2)−Cu(1)−P(2)	106.81(12)
		P(1)−Cu(1)−P(2)	126.32(5)
		N(1)−Cu(1)−N(2)	79.55(17)

Fabrication of Electroluminescent Devices. The EL device using compound **4** as the emitter was fabricated on an indium−tin oxide (ITO) substrate, which was cleaned by an ultraviolet ozone cleaner immediately before use. The solution for spin-coating was made up of the $CHCl_3$ solution of PVK and compound **4** (80:20 wt%). This solution was spin-cast onto an ITO glass at 1500 rpm. The hole-blocking layer, F-TBB (1,3,5-tris(4′-fluorobiphnenyl-4-yl)benzene), and the electron-transport layer, Alq_3, were deposited

(10) SHELXTL NT Crystal Structure Analysis Package, Version 5.10, Analytical X-ray System, Bruker AXS: Madison, WI, 1999.
(11) (a) Pålsson, L.-O.; Monkman, A. P. *Adv. Mater.* **2002**, *14*, 757. (b) Mello, J. C.; Wittmann, H. F.; Friend, R. H. *Adv. Mater.* **1997**, *9*, 230.

Chart 1

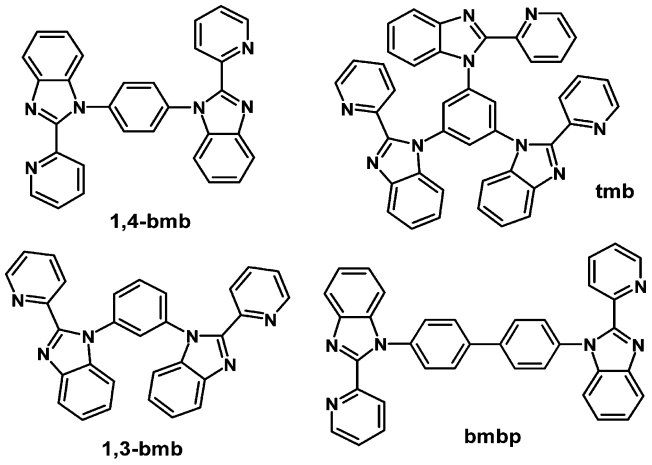

by vacuum. The cathode composed of LiF and Al was deposited on the substrate by conventional vapor vacuum deposition. The triple-layer device with the structure of ITO/PKV+ **4** (∼60 nm)/F-TBB (15 nm)/Alq_3 (15 nm)/LiF (1.0 nm)/Al (15 nm) was fabricated. The active device area is 1.0 × 5.0 mm^2. The current/voltage characteristics were measured using a Keithley 238 current/voltage unit. The EL spectra and the luminance for the devices were measured by using a Photo Research-650 Spectra Colorimeter.

Results and Discussion

Syntheses and Structures. The organic ligands used in this study are 1,4-bmb, 1,3-bmb, tmb, and bmbp, which were synthesized by using a Ullmann condensation procedure reported recently by our group.[8] The structures of these four ligands are shown in Chart 1. These molecules have been found to be excellent chelate ligands for binding to Cu(I) ions. The reactions of these ligands with the stoichiometric amount of $[Cu(CH_3CN)_2(PPh_3)_2][BF_4]$ resulted in the isolation of the corresponding yellow crystalline Cu(I) complexes, $[Cu_2(1,4\text{-bmb})(PPh_3)_4][BF_4]_2$ (**1**), $[Cu_2(1,3\text{-bmb})(PPh_3)_4][BF_4]_2$ (**2**), $[Cu_3(tmb)(PPh_3)_6][BF_4]_3$ (**3**), and $[Cu_2(bmbp)(PPh_3)_4][BF_4]_2$ (**4**), respectively in good yields. Compounds **1**−**4** are stable in solution under air. For compounds **2**−**4**, single crystals that are suitable for X-ray experiments were obtained and their structures were therefore determined by single-crystal X-ray diffraction analysis.

The structure of the cation in **2** is shown in Figure 1. The Cu(I) ion has an approximately tetrahedral geometry with two terminal PPh_3 ligands and one 2-(2′-pyridyl)benzimidazolyl chelate. There is a distinct difference between the two Cu−N bond lengths: the Cu(1)−N(1) (pyridyl) bond length (2.176(5) Å) is much longer than that of Cu(1)−N(2) (imidazolyl, 2.063(5) Å), indicating that the imidazolyl nitrogen atom is a stronger donor than that of the pyridyl ring. The same trend was also observed for the structures of **3** and **4** (see Table 2). The 2-(2′-pyridyl)benzimidazolyl chelate plane is approximately perpendicular to the central benzene plane due to steric interactions between the pyridyl ortho hydrogen atom and those of the central benzene ring. The Cu(1)−Cu(1A) separation distance is 9.82(1) Å.

The molecule of **2** possesses a crystallographically imposed C_2 symmetry. The C_2 symmetry is the consequence

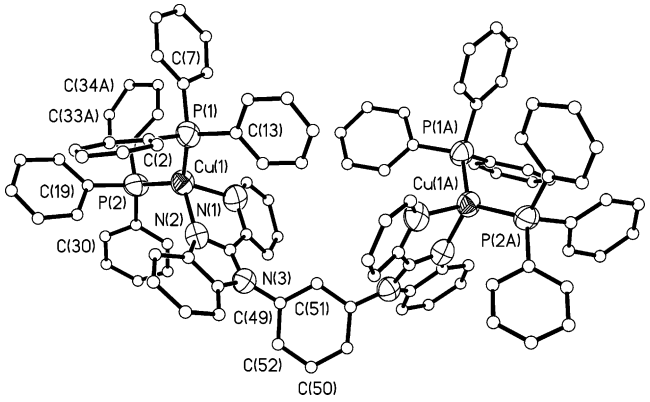

Figure 1. A diagram showing the structure of **2**. For clarity, all carbon atoms are shown as ideal spheres and all hydrogen atoms are removed. The full ellipsoid diagram can be found in the Supporting Information.

Chart 2

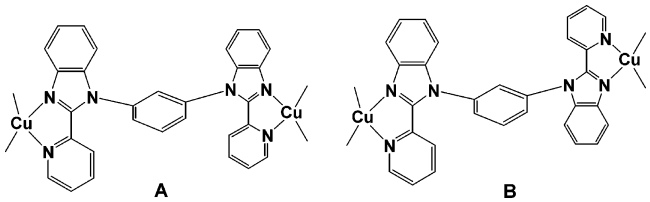

of the relative orientation of the two 2-(2′-pyridyl)benzimidazolyl groups with respect to the central benzene plane. In the crystal structure, these two units are oriented anti to each other (structure **B**, Chart 2). The other possible orientation is **A** where the two 2-(2′-pyridyl)benzimidazolyl groups have a syn arrangement and are related by a mirror plane symmetry. Although the crystal structure of **1** was not determined, similar syn and anti isomers as depicted in Chart 2 are also possible. In fact, we have observed that, for Pt(II) complexes $[(PtPh_2)_2(1,3\text{-bmb})]$ and $[(PtPh_2)_2(1,4\text{-bmb})]$, both syn and anti isomers coexist in solution at ambient temperature and they only interconvert at high temperature,[8] which was attributed to the hindered rotation of the 2-(2′-pyridyl)-benzimidazolyl chelate unit. To determine if the syn and anti isomers **A** and **B** coexist in solution for **1** and **2**, we carried out variable-temperature $^{31}P\{^1H\}$ NMR for both compounds. In the temperature range of 298−183 K, only one ^{31}P chemical shift was observed for both compounds (no free PPh_3 peak was observed), which could be explained by the existence of one isomer. On the other hand, it is also possible that the ^{31}P chemical shifts for the **A** and **B** isomers are similar, hence indistinguishable, which is in fact the case as confirmed by a variable-temperature ^1H NMR experiment. The variable-temperature ^1H NMR spectra for **1** are shown in Figure 2. At 298 K, one set of broad chemical shifts were observed for the 2-(2′-pyridyl)benzimidazolyl unit of the complex. As the temperature was lowered, two distinct sets of chemical shifts with ∼1:1 ratio were observed, which supports the coexistence of the **A** and **B** isomers in solution. The **A** and **B** isomers undergo a dynamic exchange at temperatures above 203 K. The activation energy of this exchange process for **1** was estimated[12] to be ∼61 kJ mol^{-1}

(12) Williams, D. H.; Fleming, I., *Spectroscopic Methods in Organic Chemistry*, 4th ed.; McGraw-Hill: London, 1987.

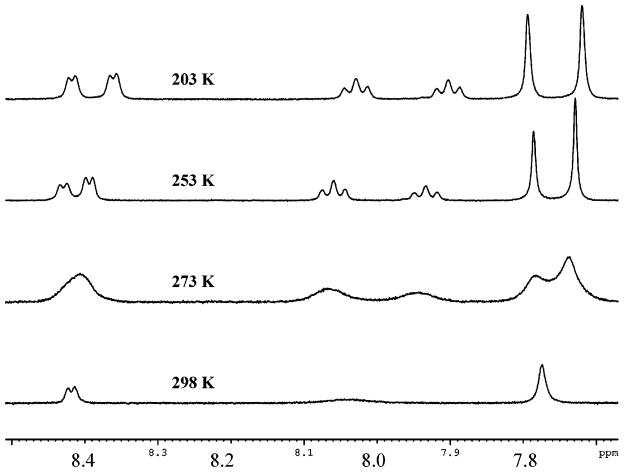

Figure 2. Variable-temperature ^{1}H NMR spectra for **1** showing part of the aromatic region.

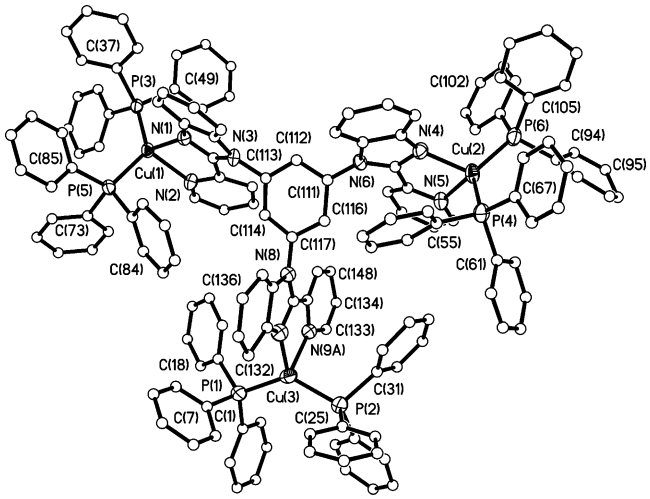

Figure 3. A diagram showing the structure of **3**. For clarity, only one orientation of the disordered groups (the N(9a) 2-Py-benzimidazolyl ring bound to Cu(3), and the C(94) phenyl ring) is shown, hydrogen atoms are omitted, and all carbon atoms are shown as ideal spheres. The complete structure with thermal ellipsoids is provided in the Supporting Information.

by using the two chemical shifts at the 7.9−8.1 ppm region and the coalescence temperature of 298 K. Variable-temperature ^{1}H NMR experiments also confirmed the coexistence of isomers **A** and **B** in solution for **2** with a similar activation energy barrier, ~62 kJ mol^{-1}.

Compound **3** contains three Cu(I) centers each of which is chelated by a 2-(2′-pyridyl)benzimidazolyl unit and further coordinated by two PPh_3 ligands in the same manner as in **2** (Figure 3). The Cu−Cu separation distances are Cu(1)−Cu(2) 12.75(1) Å, Cu(2)−Cu(3) 10.27(1) Å, and Cu(1)−Cu(3) 10.25(1) Å, respectively, which are, on average, much longer than that in **2**, clearly caused by the increased congestion of ligands in **3**. One important feature is that the 2-(2′-pyridyl)benzimidazolyl unit chelated to the Cu(3) center has two different orientations—**A** where it orients in the same direction as the other two 2-(2′-pyridyl)benzimidazolyl units and **B** where it orients in the opposite orientation with respect to the other two 2-(2′-pyridyl)benzimidazolyl units (see Chart 3). Crystallographically, this is manifested as a two-site disordering (see figures in Supporting Information). On the

Chart 3

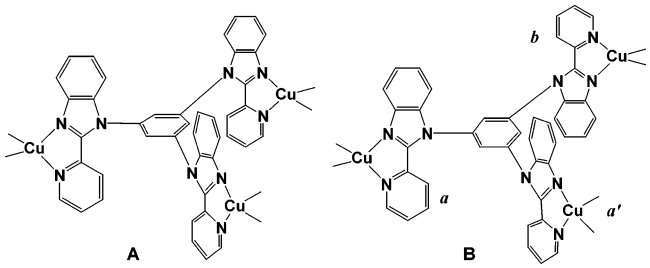

basis of the crystal structural data, we believe that compound **3** exists as a 1:1 mixture of the isomers **A** and **B** in the solid state. ^{1}H NMR study indicated that these two isomers coexist in solution and undergo interconversion at ambient temperature, which is consistent with the behavior of **2** and **3**. Due to the complexity of the ^{1}H NMR spectra of **3**, we have not been able to estimate the activation energy. Similar isomerization was also observed in the related Pt(II) compound $(PtPh_2)_3(tmb)$.[8]

The structure of compound **4** is shown in Figure 4. The molecule of **4** possesses a crystallographically imposed inversion center symmetry that relates the two Cu(1) units. The coordination environment around the Cu(I) center is similar to that observed in **2** and **3**. The Cu(1)−Cu(1A) separation distance, 17.32(2) Å, is much longer than those in **2** and **3** due to the increased length of the biphenyl linker in the ligand. Because of the free rotation around the C−C bond in the biphenyl unit, no structural isomerism similar to those observed in **2** and **3** is present for **4**.

The N−Cu−N bite angles in compounds **2**−**4** range from 76.7(5) to 80.2(2)° and the P−Cu−P bond angles from 124.66(7) to 132.93(10)°. The average (78.8°) of the N−Cu−N angles is a few degrees smaller than that[13] of $[Cu(Phen)(PPh_3)_2]^+$ (80.90(9)°), and the average (127.9°) of the P−Cu−P bond angles is much larger than that[13] of $[Cu(Phen)(PPh_3)_2]^+$ (115.44(4)°), which can be explained by the increased steric congestion in **2**−**4**.

Spectroscopic and Electrochemical Properties. The absorption spectra of the free ligands 1,4-bmb, bmbp, 1,3-bmb, and tmb are similar with two absorption bands at $\lambda_{max} \approx 230$ and 300 nm, attributed to the $\pi \rightarrow \pi^*$ transition centered on the 2-(2′-pyridyl)benzimidazolyl units.[8] In CH_2Cl_2, the absorption spectra of complexes **1**−**4** have similar features as the ligands. However, in addition to the high-energy absorption bands, all complexes have a weak and broad low-energy shoulder band in the 350−450 nm region

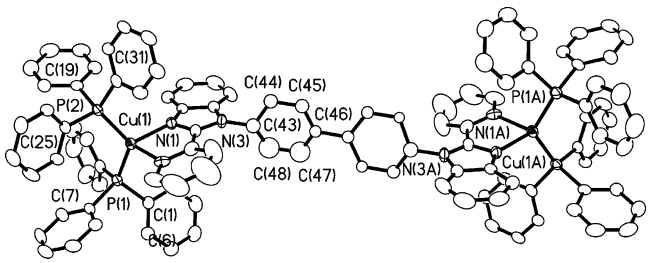

Figure 4. A diagram showing the structure of **4** with 50% thermal ellipsoids. For clarity, only one orientation of the disordered biphenyl group is shown and all hydrogen atoms are omitted. The complete diagram is provided in the Supporting Information.

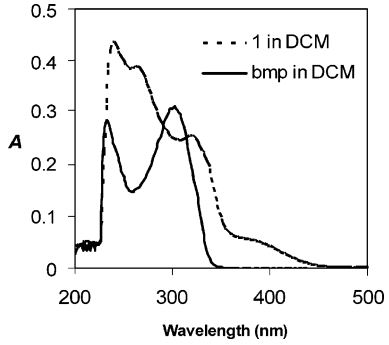

Figure 5. UV−vis spectra of bmp and the complex **1** in CH_2Cl_2.

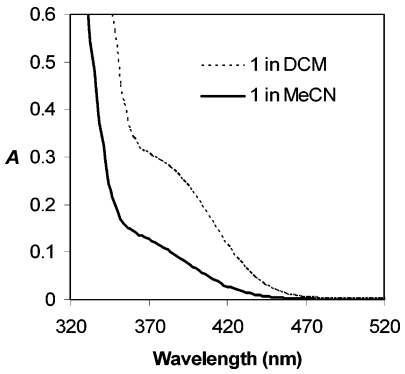

Figure 6. The MLCT region of the UV−vis spectra of **1** in CH_2Cl_2 and CH_3CN, respectively, recorded using the same concentration.

(Figure 5), which accounts for the yellow color of the complexes. This low-energy transition band resembles the MLCT band observed in[7] $[Cu(Phen)(PPh_3)_2]BF_4$. It is therefore attributed to MLCT transfer transitions involving the *N*,*N*-chelate ligand and the Cu(I) ion. The MLCT band of **1**−**4** shifts toward a shorter wavelength in the polar solvent CH_3CN, as shown by Figure 6, which is consistent with the behavior of Cu(I) phenanthroline complexes.[7]

In CH_3CN solution, complexes **1**−**4** display a broad and irreversible oxidation peak with the peak height at 1.63 (**1**), 1.67 (**2**), 1.79 (**3**), and 1.71 V (**4**), respectively. A poorly resolved shoulder peak is also observed for **1** (at ∼1.35 V) and for **4** (at ∼1.45 V). We believe that the broad oxidation peak of the complex likely involves multiple electron-transfer originating from the chelate ligand and the Cu(I) center. The electrochemical behavior of **1**−**4** resembles that of $[Cu(Phen)(PPh_3)_2]BF_4$ reported by McMillin and co-workers where a irreversible oxidation peak was observed.[7] However, the oxidation potential of the $[Cu(Phen)(PPh_3)_2][BF_4]$ complex is much lower than those observed for **1**−**4**, which indicates that the HOMO level of complexes **1**−**4** is much deeper than that of $[Cu(Phen)(PPh_3)_2]BF_4$. Furthermore, the electrochemical data appear to support that the HOMO level of the complexes has contributions from both ligand and the Cu(I) center. A reversible reduction peak at ∼2.0 V was observed for all four complexes which can be attributed to the reduction of the chelate ligand.

When irradiated by UV light, the free ligands emit a weak purple/blue color with $\lambda_{max} \approx 365-415$ nm in CH_2Cl_2

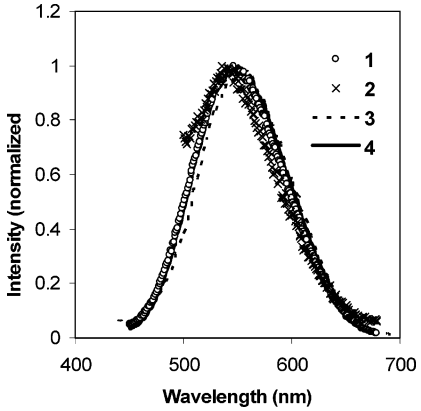

Figure 7. The emission spectra of **1**−**4** in PMMA films.

solution at ambient temperature, which were assigned to fluorescent emissions originating from a ligand-centered $\pi \rightarrow \pi^*$ transition.[8] At 77 K, a broad phosphorescent emission band for all free ligands in the 400−650 nm region with $\lambda_{max} \approx 500$ nm in CH_2Cl_2 was observed. The decay lifetime of the phosphorescent emission of the free ligands was found to be in the range of 7.0(1)−13.2(1) μs. In contrast to the behavior of the free ligands, complexes **1** and **4** display a weak yellow-orange emission in solution such as THF and CH_2Cl_2 while **2** and **3** do not have any detectable emission in solution at ambient temperature. When doped into a polymer matrix such as PVK or PMMA, these compounds display fairly bright yellow-orange luminescence when irradiated by UV light at ambient temperature. The PMMA film emission energy of **1**−**4** at ambient temperature is similar with the λ_{max} at 535−550 nm as shown in Figure 7. At 77 K, there is a 10−20 nm red shift in emission energy for the PMMA film (Table 3). The emission spectra of **1**−**4** in CH_2Cl_2 at 77 K resemble those of the PMMA film. Using an integration sphere, the absolute emission quantum yield of complexes **1**−**4** (doped in PMMA, 20%: 80 wt%) was measured to be 11%, 17%, 12%, and 15%, respectively, which are comparable to that[6] of $[Cu(Phen)(PPh_3)_2][BF_4]$ (14%). One thing we observed is that the phosphorescent emission band of the free ligands only partially overlaps with the MLCT absorption band of the metal complexes, which may explain the relatively low quantum efficiency of complexes **1**−**4**. The decay lifetimes of complexes **1**−**4** at 77 K in CH_2Cl_2 and in PMMA were determined by using a time-resolved phosphorescent spectrometers. Most the decay curves are fitted well with a single component (∼200 μs). For those that displayed a small deviation from the single-component fit, two components were used, which generated a long decay lifetime (the dominating one) and a relatively fast decay lifetime. The long decay lifetime displayed by the Cu(I) complexes, characteristic of triplet state emission, is much longer than that[6,7] of $[Cu(Phen)(PPh_3)_2][BF_4]$, which may hinder their use as emitters in EL devices.

Electroluminescent Device of 4. Compound **4** was selected as a representative example for the investigation of electroluminescent properties of the Cu(I) complexes because of its relatively high solubility, good film forming properties with PMMA, and its relatively short decay lifetime in

(13) Kirchhoff, J. R.; McMillin, D. R.; Robinson, W. R.; Powell, D. R.; McKenzie, A. T.; Chen, S. *Inorg. Chem.* **1985**, *24*, 3928.

Table 3. Absorption and Luminescent Data for **1**−**4**

comp.	absorp.,[a] nm λ_{max} (ϵ, $M^{-1}cm^{-1}$)	emiss, λ_{max}, nm in DCM[a] 77 K	emiss, λ_{max}, nm in PMMA 77 K[b]	emiss, λ_{max}, nm in PMMA rt[b]	Φ	τ (μs) in DCM 77 K	τ (μs) in PMMA 77 K
1	240 (69,694), 264 (61,156), 320 (40,851), 380 (8,394)	557	556	546	11	211(1)	196(2)
2	234 (63,104), 264 (43,878), 320 (27,730), 386 (4,668)	561	556	535	17	99(4), 279(5)	112(10), 349(17)
3	232 (93,029), 262 (72,418), 312 (38,016), 388 (5,567)	558	570	547	12	241(1)	263.4(7)
4	232 (93,813), 266 (78,507), 322 (42,322), 380 (8,271)	561	563	550	15	74(5), 220(7)	188(1)

[a] $[c] = 10^{-5}$ M. [b] 20 wt% in PMMA.

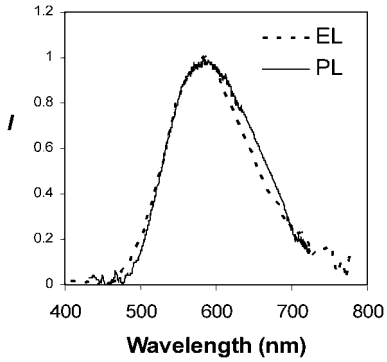

Figure 8. The PL spectrum of **4** in PVK and the EL spectrum of the device.

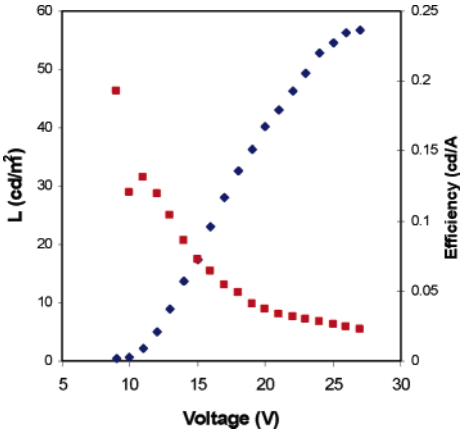

Figure 9. The $L-V$ and current efficiency$-V$ characteristics of the EL device.

PMMA, compared to compounds **1**−**3**. The EL device was fabricated by spin-coating a compound **4**/PVK blend (20:80 wt%) in CH_2Cl_2 to the ITO substrate. The choice of PVK as the host material is based on the fact that PVK is an excellent hole transport molecule and its emission band is near 400 nm, which overlaps with the MLCT absorption band of complex **4**. A hole blocking layer F-TBB to prevent the exciton formation within the Alq_3 layer (F-TBB = 1,3,5-tris(4′-fluorobiphnenyl-4-yl)benzene, 15 nm) was deposited on top of the **4**/PVK layer by vacuum deposition. The electron transport layer Alq_3 (15 nm) was deposited on top of the F-TBB layer by vacuum. Finally, the cathode layer LiF (1 nm) and Al (15 nm) were deposited on top of the organic layers by thermal evaporation. The device produced a orange emission which matches very well with the PL spectrum of the **4**/PVK blend film ($\lambda_{max} = 580$ nm), as shown in Figure 8. No PVK or Alq_3 emission was observed. However, as shown by the $L-V$ and the current efficiency$-V$ data in Figure 9, the EL device of **4** is not bright and the efficiency is low. The long decay lifetime of the triplet state emission and the relatively low photoluminescent quantum efficiency of compound **4** may be partially responsible for the low EL efficiency of the device. As noted by Wang and co-workers, the EL performance of [Cu(Phen)(DPEphos)][BF_4], DPEphos = bis[2-(diphenylphosphino)phenyl]ether, is much better than that of [Cu(Phen)(PPh_3)$_2$][BF_4] due to its increased quantum efficiency and the shortened decay lifetime.[6] We are currently investigating if the replacement of the PPh_3 ligand by the DPEphos ligand can significantly improve the properties of our Cu(I) complexes and the details will be published in due course. The exceptionally long decay lifetime of complexes **1**−**4** is clearly associated with the 2-(2′-pyridyl)benzimidazolyl unit. Therefore, to dramatically improve the performance of the EL devices, further chemical modifications on the chelate ligands are necessary.

In summary, four dinuclear and trinuclear Cu(I) complexes based on bmb, tmb, and bmbp ligands that either display a linear shape or a star shape have been synthesized and fully characterized. These complexes have a good stability in solution and in the solid state. Except complex **4**, which has a 4,4′-biphenyl linker in the chelate ligand, these complexes display syn and anti structural isomerism caused by the hindered rotation of the 2-(2′-pyridyl)benzimidazolyl chelate unit. Isomer interconversion occurs in solution at ambient temperature. Yellow-orange luminescence due to MLCT transitions has been observed for all complexes. These new complexes display exceptionally long decay lifetimes which may hinder their uses as emitters in EL devices as demonstrated by the poor performance of the EL device based on complex **4**. On the other hand, the long decay lifetime of **1**−**4** may render them as good candidates for photochemistry applications, which will be examined in our laboratory.

Acknowledgment. We thank the Nature Sciences and Engineering Research Council of Canada for financial support.

Supporting Information Available: ^1H NMR spectra of complexes **2** and **3** at ambient and low temperature, complete crystal structural diagrams with labeling and X-ray diffraction data for **2**−**4**, including tables of atomic coordinates, thermal parameters, bond lengths and angles, and hydrogen parameters. This material is available free of charge via the Internet at http://pubs.acs.org.

IC0504893